# **CHAPTER 164**

DECOUPLED NUMERICAL MODEL OF THREE-DIMENSIONAL BEACH CHANCE

Magnus Larson<sup>1</sup>, Nicholas C. Kraus<sup>2</sup>, M.ASCE, and Hans Hanson<sup>3</sup>

### ABSTRACT

This paper describes a numerical model of three-dimensional beach change as produced by breaking waves and wave-induced currents. Cross-shore lines spaced at intervals alongshore form the basic calculation element, and cross-shore and longshore transport rates are calculated independently on the lines. Transport rates are coupled indirectly through the mass conservation equation and a contouring routine that determines local depth contour orientation for calculating wave transformation. The model has reduced calculation time compared to fully gridded hydrodynamic and beach change models, yet allows representation of complex boundary conditions, coastal structures, and movement of longshore bars and berms. Results of two test series are presented, one for the movement and protective functioning of a linear mound constructed of dredged material, and the other for impoundment at a jetty.

### INTRODUCTION

The goal of beach change numerical modeling is to describe the threedimensional (3D) evolution of nearshore bottom topography resulting from spatial and temporal differences in sand transport. For practical use, five model capabilities were considered to be essential: (1) accurate and reliable beach change simulation compatible with input data routinely available at engineering projects; (2) representation of sand transport and beach change on temporal and spatial scales of engineering interest; (3) representation of general boundary conditions and coastal structure configurations; (4) calculation robustness, meaning that uncertainties typically present at projects do not produce

<sup>(1)</sup> Assist. Prof., (3) Assoc. Prof., Dept. of Water Resources Engrg., Institute of Technol., Univ. of Lund, Box 118, Lund, Sweden S-221 00. (2) Sr. Res. Sci., Coastal Engrg, Res. Center, U.S. Army Engr. Waterways Experiment Station, 3909 Halls Ferry Road, Vicksburg, MS 39180-6199.

aberrant model predictions; and (5) economical execution time. The second capability implies that both short-term processes (e.g., storm-induced beach erosion/recovery, and cyclical daily and seasonal change in the beach profile shape and position) and long-term processes (e.g., accretion and erosion at shore-normal structures) are simulated, including approach to an equilibrium bottom configuration under constant forcing and boundary conditions. A model having these capabilities is now under development, and this paper introduces the model and representative initial test results.

### Model Architecture

To develop a 3D bathymetric change numerical model with the aforementioned five capabilities for wide-application use, the model architecture was founded on two design concepts. The first concept was to combine essential features of two previous successful beach change models, SBEACH for calculating storm-induced beach erosion and recovery (Larson et al. 1988, Larson and Kraus 1989, Larson et al. 1990) and GENESIS for calculating long-term change in shoreline position (Hanson 1989, Hanson and Kraus 1989). The 3D modeling system also allows extension of capabilities of the two models that is not possible within the limits of the individual models. The second design concept was to treat lines running across the shore as the basic calculation element. Waves, longshore current, and longshore and cross-shore transport rates are calculated independently on the cross-shore lines, decoupling the transport rate calculation along the beach. Neighboring areas of the beach interact through a local contouring routine that calculates the beach orientation at each grid point on the cross-shore lines and through the sand mass conservation equation, from which the change in bathymetry is obtained from the transport rates.

The resultant model, called 3DBEACH for  $\underline{3}$ -dimensional  $\underline{D}$ ecoupled model of  $\underline{BEA}$ ch  $\underline{CH}$ ange, is significantly more efficient than "point models" that require computation-intensive and sophisticated 2D gridded hydrodynamic wave and current models, yet it gives stable, equilibrium beach profile shapes that are difficult to attain in point models. Despite the simplification introduced by the decoupling approach, the model has substantial generality in representation of profile shape, such as multiple bars and troughs, than allowed in "line models" that require monotonically increasing depth with distance offshore.

By decoupling cross-shore and longshore transport processes, execution time is minimized, allowing the model to be applied either on the local or regional level and for long simulation times. The local validity of the cross-shore line as the basic calculation element restricts model applications to situations with mild bottom slopes alongshore; also, partially enclosed embayments where the shoreline intersects a cross-shore line more than once cannot be represented. Thus, 3DBEACH is targeted toward the open coast, and local bathymetric disturbances such as rip currents and rip channels are not represented directly.

#### Model Structure

3DBEACH consists of six calculation modules that function semi-independently, allowing modification of any module without affecting or requiring detailed knowledge of the other modules. Principal quantities calculated by the respective modules are: (1) wave height, wave angle, mean water level, and runup; (2) longshore current; (3) cross-shore sand transport rate; (4) longshore sand transport rate; (5) bottom contour orientation; and (6) bottom topography change.

Fig. 1 is a schematic of a 3DBEACH calculation grid. A Cartesian coordinate system is placed on the project coast with the x-axis pointing offshore and the y-axis following the trend of the shoreline. Cross-shore lines are placed along the coast with an interval  $\Delta y$ , and grid points on the line are spaced  $\Delta x$  apart. Typically,  $\Delta y$  is much larger than  $\Delta x$  under the assumption that the beach slope changes much more gently alongshore than across-shore. Fine grid spacing across-shore (typically 1 to 5 m) is needed to describe dominant morphological profile features such as bars, troughs, berms, and rapid change occurring during storms, whereas a coarse spacing alongshore (typically 25 to 100 m) is compatible with more gradual beach change produced by gradients in longshore sand transport. A time step in the range of 5 to 40 min is used in the model, with a typical value of 20 min. Short descriptions of the six calculation modules follow.

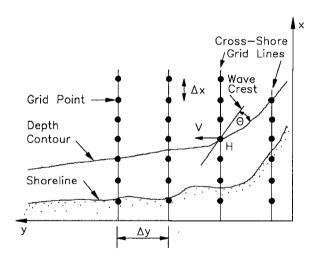


Fig. 1. Schematic of a 3DBEACH calculation grid

(1) Wave module. The wave module calculates the wave height H and other wave-related quantities, such as wave angle  $\theta$  and wave- and wind-induced setup, at grid points on each profile line (Kraus and Larson 1990). Cell opening (wetting) and closing (drying) occurs according to the wave and wind conditions, and tide level. Assuming locally plane and parallel depth contours the wave height is determined by linear

wave theory in regions of nonbreaking and by the Dally et al. (1985) model where waves break. Either regular or random wave height can be specified. The module reproduced wave breaking and reformation over bar and trough profiles measured in a large wave tank (Kajima et al. 1982), as well as wave height and setup in laboratory experiments with a plane beach and oblique wave incidence (Visser 1982). The wave module only requires input time series of wave height, period, and direction (and wind speed and direction if wind is important).

- (2) Longshore current module. The longshore current V is calculated at grid points on each cross-shore line as in the model NMLONG (Kraus and Larson 1990, Larson and Kraus 1991b). NMLONG was developed to calculate the longshore current over a multiple bar and trough profile produced by oblique wave incidence and wind, and it contains linear or nonlinear bottom friction as options, and lateral mixing. The model was verified using two field data sets (Kraus and Sasaki 1979, Thornton and Guza 1986) and one laboratory data set (Visser 1982), and default values of empirical parameters are provided. The longshore current is used to calculate the longshore sand transport rate.
- (3) Cross-shore transport module. The net cross-shore sand transport rate on each cross-shore line is calculated as in SBEACH (Larson and Kraus 1989). The profile is divided into four zones of different wave and transport properties, with the magnitude of the transport mainly governed by energy dissipation in the surf zone. SBEACH has been verified with data both from large wave tank experiments and the field (Larson and Kraus 1989, 1991a, Larson et al. 1990). The calculation procedure can generate bars and berms, but at present it is restricted to cross-shore transport related to breaking waves. The wave module supplies the main input to this module, which also requires an initial profile shape and sediment grain size.
- (4) Longshore transport module. A local transport rate formula proposed by Kraus et al. (1988) based on field measurements is used, in which the needed longshore current velocity and wave height are obtained from modules (1) and (2). Inputs are supplied by the wave and longshore current modules. This module contains an empirical transport rate parameter that must be determined in calibration.
- (5) Contour module. The orientation of depth contours is required to define a local wave angle to determine the magnitude and direction of the longshore transport. The contour orientation at each grid point is obtained by approximating the local bathymetry with a plane. The calculation requires depths from neighboring cross-shore lines and provides indirect interaction among the lines.
- (6) Bottom change module. Changes in the bottom topography are obtained from the mass conservation equation after the cross-shore and longshore transport rates have been calculated at each grid point for the particular time step.

#### MODEL TESTS

Results of two of many model test series are described. The objective of these initial "proof of concept" tests was demonstration of correct qualitative behavior for simulating realistic project conditions. One series focused on the response of a subaqueous mound of dredged material and the feedback to the waves, current, and beach from the mound. The other series focused on impoundment at a jetty or groin. In the simulations, if a random wave input time series was used, the wave height and/or angle were uniformly distributed over a given interval. The longshore grid spacing varied between 20 and 50 m, and the cross-shore spacing varied between 2 and 5 m, depending on the test. The time step was fixed at 20 min.

### Placed Mound (Silver Strand, Calif.)

Simulation conditions pertain to a Corps of Engineers project at Silver Strand Beach, California, located south of San Diego Harbor (see Junke et al. 1989). In December 1988, approximately 80,000 cu m of sand with median diameter 0.18 mm were dredged from the harbor entrance channel and placed offshore of Silver Strand in the form of a short linear mound on the existing bottom of 0.25-mm sand. The mound was intended to break higher, potentially erosive waves, as well as nourish the beach by onshore migration. The mound was initially 381 m long and 76 m wide, extending from about 225 m to 450 m from the shoreline (between bottom contours of 4.5 and 9 m), and with an average relief of 2.1 m at its crest. The bathymetry was surveyed periodically for two years on seven profile lines spaced at 76-m intervals, five lines on the feature and two to the south (historic direction of littoral movement alongshore). The bathymetry shortly after construction of the feature was completed is shown in Fig. 2. This configuration served as the initial condition for this model test series.

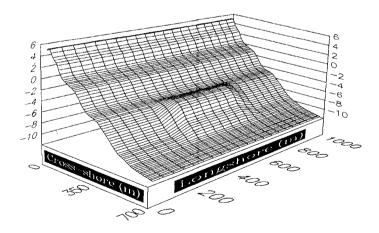


Fig. 2. Initial bathymetry for offshore mound test series

Four tests distinguished by input wave conditions are presented: (1) moderately erosional waves; (2) storm with shore-normal approach; (3) storm with oblique approach; and (4) accretionary waves. A semidiurnal tide with amplitude of 0.56 m (mean amplitude for Silver Strand) was applied in all tests, and calculations were carried out for simulated times of 3 to 10 days. A pinned-beach boundary condition (Hanson and Kraus 1989) was specified at both sides of the grid, whereby sand could freely enter and leave the calculation domain from the lateral boundaries. The cross-shore lines ended in a depth of 11.4 m, necessary to ensure that negligible transport occurred at the seaward boundary, even under storm waves. The net direction of transport as erosive (offshore directed) or accretionary (onshore directed) is determined in the model according to the criterion used in SBEACH (Larson et al. 1988, Larson and Kraus 1990) that has subsequently been further verified with a large field data set (Kraus et al. 1991).

Test 1: Moderately erosive waves. Fig. 3 displays simulation results after exposure of the coast to moderately erosional waves for 10 days. The deepwater wave height  $\rm H_{O}$  randomly varied between 1 and 2 m, the wave period T was 12 sec, and the incident deepwater wave angle  $\theta_{O}$  randomly varied between -10 and +10 deg. Because of their relatively small height, the waves passed over the mound with little change and broke further inshore. The waves gradually removed material from the foreshore and deposited it shoreward of the mound to produce an almost uniform longshore bar. This storm bar has distinct depressions resulting from refraction at the ends of the mound. Mound end effects also produce depressions on the foreshore.

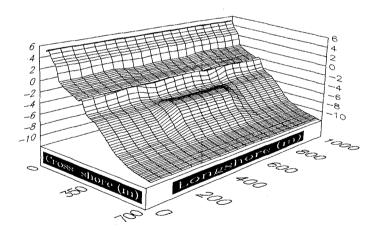


Fig. 3. Bar formation and beach erosion by moderately erosive waves

<u>Test 2: Strong storm, normal wave incidence</u>. It is of considerable interest to quantitatively evaluate the protection afforded by a mound to the beach in its lee. Thus, simulations were conducted for a 3-day

storm with  $H_{\rm O}$  randomly varying between 4 and 6 m and T = 12 sec, with the waves incident normal to the mound. Fig. 4 shows the bathymetry at the end of the storm, in which a pronounced and curved longshore bar is seen. The shape of the mound significantly changed because the waves breaking on its seaward side moved material from the mound offshore to form part of the bar. At the sides of the mound the bar lies closer to shore because material forming it had to be taken from the inner surf zone, whereas the mound supplied sand to the erosive waves breaking directly seaward of it. The mound therefore protected the beach and surf zone directly shoreward of it, both satisfying the demand for sand by the breaking waves in development of the storm bar and by causing additional wave breaking. The sand supplied by the mound replaced that taken from the surf zone in the regions on the sides of the mound, as seen by the more seaward movement of contour lines on the unprotected sides. The beach face does not show significant change alongshore, because erosion on the foreshore is strongly controlled by water level, and not depth-limited breaking waves. The complete symmetry of the calculation with respect to a shore-normal line at the center of the mound is an indication of the stability of the calculation.

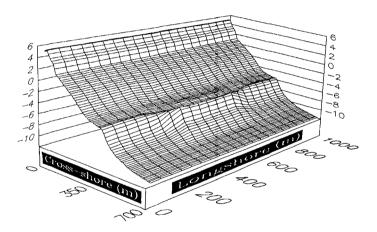


Fig. 4. Bathymetric change for a storm, normally incident waves

Test 3: Strong storm, oblique wave incidence. The previous test, a strong storm, was repeated, but with  $\theta_{\rm o}$  varying between 0 and 20 deg to introduce net longshore transport. Fig. 5 shows that the bathymetric response is no longer symmetric as in Test 2. Because of wave refraction, the longshore sand transport rate was reduced at the downdrift end of the mound; a local depth maximum appeared downdrift of the mound, further modifying the wave transformation. The present test produced satisfactory results; however, in related tests examining sensitivity to incident wave angle, if a large oblique angle was maintained for a long time interval, the greatly changing bathymetry induced numerically-generated rhythmic features. In such extreme cases,

decoupling of the cross-shore lines was not satisfactory because the longshore depth gradients were not small.

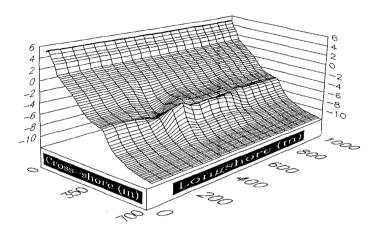


Fig. 5. Bathymetric change for a storm, obliquely incident waves

Test 4: Accretionary waves. Simulations with low waves were conducted to calculate the response of the beach and mound to accretionary forcing conditions. Such conditions occur in the summer (in the northern hemisphere) and after storms, when low waves of long period typically arrive. Fig. 6 shows the results of one such test performed with  $\rm H_{\rm O}$  varying between 0.6 and 0.8 m, T = 14 sec, and the  $\rm \theta_{\rm O}$  varying between 0 and 20 deg. The waves were run for 10 days. The mound shape was only slightly altered by the low waves which passed over it and travelled shoreward to break in shallower water. A distinct berm formed on the foreshore that is not uniform alongshore due to refraction of the incident waves at the mound.

#### Impoundment at Jetty

This test series examined model predictions for impoundment at a jetty or groin. Two tests are described which exercised the "groin boundary condition," one without bypassing and the other including bypassing. Mildly erosional monochromatic waves were applied ( $H_0=2$  m, T=8 sec,  $\theta_0=20$  deg). Similar calculations performed with random waves did not change the essential features of the bathymetric response, randomness only acting to produce a smoother topography. Fig. 7 shows the initial bathymetry for the groin test series, consisting of a groin situated on a plane-sloping profile joining an equilibrium ( $x^{2/3}$ ) profile at the still-water shoreline. The tide was semidiurnal with an amplitude of 0.5 m, and the area was exposed to 3 days of wave action.

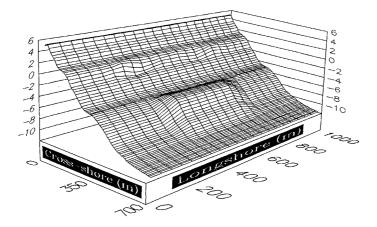


Fig. 6. Bathymetric change for accretionary waves

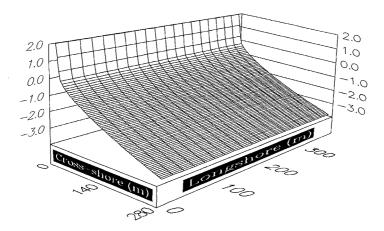


Fig. 7. Initial bathymetry for jetty test series

Infinitely long jetty. Fig. 8 shows impoundment by a long jetty (long with respect to the width of the surf zone) located on the right side of the grid. The jetty acts to completely block sand moving toward it. A longshore bar formed with its crest curving offshore with approach toward the jetty from the updrift coast. A plateau more gently sloping than the initial beach formed in the vicinity of the jetty; its buildup continued to the high-tide water level if the simulation was run for a very long time. The time scale of the beach response here and in other tests is controlled by empirical coefficients that enter as factors in the cross-shore and longshore transport rate predictive

relations. These two coefficients must be determined by model calibration at the project site.

Bypassing at jetty. For this test the jetty was terminated at the initial 2-m depth contour. The incident waves broke at approximately this depth, but the changing tide moved the break point seaward and shoreward of this contour. The longshore sand transport rate tailed off seaward of the break point in accordance with the tail in the longshore current. Sand that was transported alongshore seaward of the tip of the jetty was allowed to pass the jetty as an implementation of a simple boundary condition representing bypassing. As shown in Fig. 9, for these conditions, the bar was almost straight alongshore because the jetty did not extend to where the bar developed. The jetty still impounded sand and a gently sloping plateau developed near it, but the plateau extended only to the end of the structure.

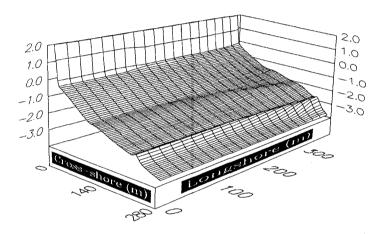


Fig. 8. Impoundment at a long jetty (no bypassing)

Additional simulations were carried out for a long jetty, encompassing 10 days of wave action ( $\rm H_{\rm O}=1$  m, T = 8 sec,  $\theta_{\rm O}=20$  deg), which illustrates the equilibrium properties of 3DBEACH. Fig. 10 shows the time evolution of the profile line located closest to the groin and how the sand build-up occurs along the groin. The accumulation of sand on the updrift side of the groin will continue as long as the waves have a predominant direction. However, as the beach contours adjust towards a position where they are parallel to the incident wave crests, the sand transport decreases and the rate of accumulation becomes smaller. Thus, the model correctly describes the equilibrium characteristics of a beach with groins observed in the laboratory and field.

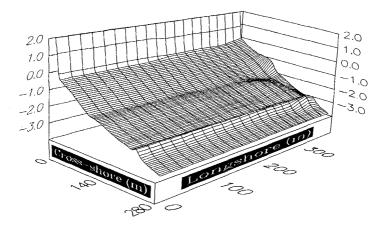


Fig. 9. Impoundment at a jetty with bypassing

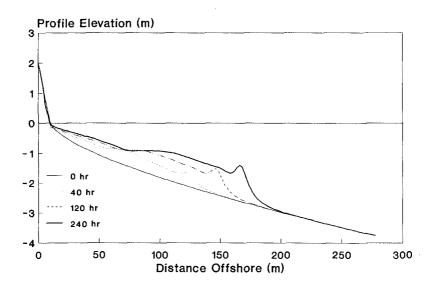


Fig. 10. Profile evolution immediately updrift an infinitely long jetty CONCLUDING DISCUSSION

This paper described initial tests of a new class of numerical model of three-dimensional beach change. The distinguishing characteristic of the model is decoupling of wave, current, and sediment transport processes on cross-shore lines spanning the nearshore. The decoupling

approximation reduces calculation time significantly over beach change models using full two-dimensional wave and current calculation schemes, yet still describes morphologic nearshore profile features of engineering interest. The model is expected to be valid if longshore bathymetry gradients are small and significantly less than cross-shore gradients.

The model presently describes sediment transport and beach change in and around the surf zone as produced by breaking waves. Because the model calculates process-driven sediment transport rates and uses the mass conservation equation to determine beach change, inclusion of non-breaking wave sediment transport generating mechanisms is possible and will be incorporated in the next phase of the study.

The tests series demonstrated that the model can describe changes in large-scale morphologic features such as breakpoint bars, berms, and plateaus formed near structures. Important features of the model are a stable approach to an equilibrium bottom configuration under steady waves and ease of implementing boundary conditions. Without possessing a regular approach to equilibrium, both the time scale and reliability of model predictions would be ambiguous. Such properties were well studied in the beach change modeling technology underlying 3DBEACH (Kraus and Larson 1988, Hanson and Kraus 1989, Larson and Kraus 1989).

#### ACKNOWLEDGEMENTS

The work carried out by ML and HH was funded through the U.S. Army Research, Development and Standardization Group, UK, under contract DAJA-88-C0015. This support is gratefully acknowledged. The contribution of NCK was performed as part of the activities of the Calculation of Boundary Properties (Noncohesive Sediments) work unit of the Dredging Research Program, US Army Corps of Engineers. Permission was granted by the Chief of Engineers to publish this information.

## REFERENCES

- Dally, W. R., Dean, R. G., and Dalrymple, R. A. 1985. "Wave height variation across beaches of arbitrary profile," <u>J. Geophys. Res.</u>, 90 (C6), pp 11917-11927.
- Hanson, H. 1989. "GENESIS A generalized shoreline change numerical model," <u>J. Coastal Res.</u>, Vol 5 (1), pp 1-27.
- Hanson, H. and Kraus, N. C. 1989. "GENESIS: Generalized model for simulating shoreline change. Report 1: Technical reference," Tech. Rep. CERC-89-19, Coastal Engrg. Res. Center, U.S. Army Engr. Waterways Expt. Station, Vicksburg, MS.
- Junke, L., Mitchell, T., and Piszker, M. J. 1989. "Construction and monitoring of nearshore disposal of dredged material at Silver Strand State Park, San Diego, California," <u>Proc. 22nd Annual</u> <u>Dredging Seminar</u>, Texas Engrg. Expt. Station, CDS Rep. No. 317, pp 203-217.
- Kajima, R., Saito, S., Shimizu, T., Maruyama, K., Hasegawa, H., and Sakakiyama, T. 1983. "Sand transport experiments performed by using a large water wave tank," Data Rep. No. 4-1, Central Res. Institute for Electric Power Industry (in Japanese).

- Kraus, N. C., Gingerich, K. J., and Rosati, J. D. 1988. "Toward an improved empirical formula for longshore sand transport," <u>Proc.</u> <u>21st Coastal Engrg. Conf.</u>, ASCE, pp 1182-1196.
- Kraus, N. C., Kriebel, D. L., and Larson, M. 1991. "Evaluation of beach erosion and accretion predictors," <u>Proc. Coastal Sediments '91</u>, ASCE.
- Kraus, N. C. and Larson, M. 1990. "NMLONG: Numerical model for simulating the longshore current," Tech. Rep., Coastal Engrg. Res. Center, U.S. Army Engr. Waterways Expt. Station, Vicksburg, MS, (in prep.).
- Kraus, N. C. and Sasaki, T. O. 1979. "Influence of wave angle and lateral mixing on the longshore current," <u>Marine Science Communications</u>, Vol 5 (2), pp 91-126.
- Larson, M. and Kraus, N. C. 1989. "SBEACH: Numerical model for simulating storm-induced beach change. Report 1: Theory and model foundation," Tech. Rep. CERC-89-9, Coastal Engrg Res. Center, U.S. Army Engr. Waterways Expt. Station, Vicksburg, MS.
- Larson, M. and Kraus, N. C. 1991a. "Mathematical modeling of the fate
   of beach fill," <u>Coastal Engrg.</u>, Special Issue on Beach Fill, (in
   press).
- Larson, M. and Kraus, N. C. 1991b. "Numerical model of longshore current for bar and trough beaches," <u>J. Waterway, Port, Coastal, and Ocean Engrg.</u>, ASCE, (in press).
- Larson, M., Kraus, N. C., and Byrnes M. R. 1990. "SBEACH: Numerical model for simulating storm-induced beach change. Report 2: Numerical formulation and model test," Tech. Rep. CERC-89-9, Coastal Engrg. Res. Center, U.S. Army Engr. Waterways Expt. Station, Vicksburg, MS.
- Larson, M., Kraus, N. C., and Sunamura, T. 1988. "Beach profile change:
   Morphology, transport rate, and numerical simulation," <u>Proc. 21st Coastal Engrg. Conf.</u>, ASCE, pp 1295-1309.
  Thornton, E. B. and Guza, R. T. 1986. "Surf zone longshore currents and
- Thornton, E. B. and Guza, R. T. 1986. "Surf zone longshore currents and random waves: Field data and models," <u>J. Phys. Oceanography</u>, Vol 16, pp 1165-1178.
- Visser, P. J. 1982. "The proper longshore current in a wave basin," Rep. No. 82-1, Dept. of Civil Engrg., Delft Univ. of Techn., Delft.